Frequency Response Analysis of Nonisothermal Film Blowing Process Using Transient Simulations

Hyung Min Kim,[1] Joo Sung Lee,[2] Hyun Wook Jung,[1] Jae Chun Hyun[1]

[1]*Department of Chemical and Biological Engineering, Korea University, Seoul 136-713, Korea*
[2]*Battery R&D, LG Chem/Research Park, Daejeon 305-380, Korea*

Received 9 December 2010; accepted 26 May 2011
DOI 10.1002/app.34987
Published online 1 September 2011 in Wiley Online Library (wileyonlinelibrary.com).

ABSTRACT: Frequency response of the nonisothermal viscoelastic film blowing process to the ongoing sinusoidal disturbances has been investigated using transient simulation techniques. Of the many state variables exhibiting resonant peaks with the input frequency, amplitude ratio of the film cross-sectional area at the freezeline height has been used as an indicator of the process sensitivity. The effects of operating conditions and viscoelasticity on the sensitivity have been scrutinized around the middle point of three multiple steady states under the given conditions. The sensitivity results have been interpreted through their correlation with results from linear stability analysis. Increasing draw ratio generally makes the system more sensitive to sinusoidal disturbances, whereas the cooling induces more sensitive or less sensitive system, according to the location of a steady state. Also, the viscoelasticity makes the system of extensional thickening fluids more sensitive at low Deborah number and less sensitive at high Deborah number. © 2011 Wiley Periodicals, Inc. J Appl Polym Sci 123: 3028–3035, 2012

Key words: film blowing; sensitivity; frequency response; PTT fluids; transient simulation

INTRODUCTION

Film blowing is an industrially important process in the fabrication of thin plastic films with biaxial orientation. It involves stretching polymer melts in both axial and circumferential directions (Fig. 1). The molten polymer is extruded through an annular die, and then stretched upwards by nip rolls, i.e., axial extension. Concurrent circumferential extension of the film occurs through its inflation by the injection of air via a hole at the center of the die. An external airflow, which is one of the major operating conditions, supplied from a concentric outer ring cools down the film.

Mathematical modeling for the steady analysis of film blowing process was pioneered by Pearson and Petrie[1,2] for an isothermal Newtonian fluid. Since then, much work, both theoretical and experimental, has shed light on the dynamics of this complex process.[3–23] Transient responses during film blowing operation were studied intensively by Pirkle and Braatz[12] group that successfully established transient routes between two steady states and systematically explained the effects of oscillating heat transfer, bubble pressure, and machine tension on film thickness. Also, they recently introduced multiplicity and instability in film blowing process accompanied with crystallization kinetics using the linear stability and transient simulation of thin-shell model, emphasizing the role of cooling or heat transfer coefficient.[15] Hyun and coworkers[18–22] solved periodic draw resonance instability for nonisothermal viscoelastic cases with or without crystallization effect that incorporated the orthogonal collocation on finite elements (OCFE), which quite well predicted experimentally observed unstable phenomena. Stability windows for various fluids can be established from linear stability work.[3,4,10,16,19,20,23] Cain and Denn[4] presented detailed stability windows for Newtonian and Maxwell fluids under different boundary condition sets. Yoon and Park[16] first reported the stability of multilayer blown films comprising Newtonian and viscoelastic fluids. Housiadas et al.[23] elucidated the stability changes by imposing both axisymmetric (varicous mode) and nonaxisymmetric (sinuous mode) infinitesimal disturbances to linearized film blowing systems.

Also, understanding how the unexpected disturbances can affect film blowing system is important for ensuring good film quality and processability. Many kinds of disturbances which might be inevitably introduced even during stable operations can

Correspondence to: H. W. Jung (hwjung@grtrkr.korea.ac.kr).

Contract grant sponsor: Mid-career Researcher Program through the NRF grant by the MEST; contract grant number: R01-2008-000-11701-0.
Contract grant sponsor: Industrial Strategic Technology Development Program; contract grant number: 10035163.
Contract grant sponsor: Korea Institute of Energy Technology Evaluation and Planning (KETEP).

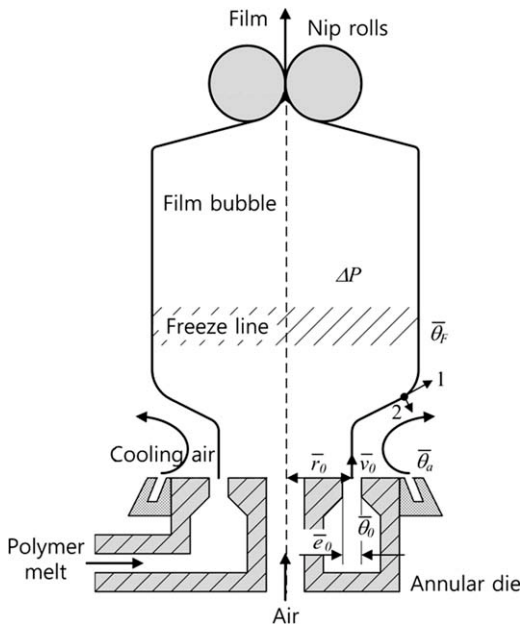

Figure 1 Schematic diagram of film blowing process.

drastically influence the stable film blowing system. For instance, in the case that air amount confined inside the inflated bubble or take-up speed or cooling (i.e., heat transfer coefficient) changed in some way due to imperfect operations, one should immediately clarify causes leading to the nonuniform products.[13,15,22] Such sensitivity is typically interpreted through the frequency response methods that measure the amplitude of sinusoidal outputs (e.g., film thickness, blow-up ratio, or cross-sectional area) with respect to a sinusoidal disturbance. Variation of the output state variables depends on the frequency and type of an imposed disturbance. Their responses obtained from linearized sensitivity[24–30] or direct transient simulation[31] methods are plotted against frequency in a Bode diagram. Sensitivity studies have been extensively carried out in fiber spinning processes, since the first reports by Denn[24] and Kase and Araki.[25] Compared to the fiber spinning case,[24–30] there have been few reports on the sensitivity of film blowing process because of its complicated dynamics. McHugh and coworkers[10,29] eloquently explained the effect of crystallization on the sensitivity using a two-phase fluid model. However, there remain some issues regarding sensitivity to elucidate the role of process conditions such as viscoelasticity, multiplicity, cooling, etc.

In this study, employing transient simulation technique devised by Hyun et al.,[18] frequency response method has been applied to investigate the sensitivity of nonisothermal film blowing process with respect to ongoing sinusoidal disturbances. Sensitivity trends of the steady-state point in the BUR (blow-up ratio)-TR (thickness reduction) diagram under several process conditions have been correlated with the stability of the system.

TIME-DEPENDENT GOVERNING EQUATIONS OF NONISOTHERMAL FILM BLOWING

The dimensionless governing equations of the nonisothermal film blowing incorporated with viscoelastic Phan-Thien and Tanner (PTT) fluids[32] are shown below, based on the work of Shin et al.[20]

Equation of continuity:

$$\frac{\partial}{\partial t}\left(re\sqrt{1+(\partial r/\partial z)^2}\right)+\frac{\partial}{\partial z}(rev)=0. \tag{1}$$

where $r=\frac{\bar{r}}{\bar{r}_0},\ e=\frac{\bar{e}}{\bar{e}_0},\ v=\frac{\bar{v}}{\bar{v}_0},\ z=\frac{\bar{z}}{\bar{r}_0},\ t=\frac{\bar{t}\bar{v}_0}{\bar{r}_0}$.

Axial force balance:

$$\frac{2re\sigma_{11}}{\sqrt{1+(\partial r/\partial z)^2}}+B\left(r_f^2-r^2\right)=T_z. \tag{2}$$

where $T_z=\frac{\bar{T}_z}{2\pi\eta_0\bar{e}_0\bar{v}_0},\ \Delta P=\frac{A}{\int_0^{\bar{z}_L}\pi\bar{r}^2d\bar{z}}-P_a, B=\frac{\bar{r}_0^2\Delta P}{2\eta_0\bar{e}_0\bar{v}_0},$ $\sigma_{ij}=\frac{\sigma_{ij}\bar{r}_0}{2\eta_0\bar{v}_0}$.

Circumferential force balance:

$$B=\left(\frac{-e\sigma_{11}\left(\partial^2r/\partial z^2\right)}{\left[1+(\partial r/\partial z)^2\right]^{3/2}}+\frac{e\sigma_{33}}{r\sqrt{1+(\partial r/\partial z)^2}}\right). \tag{3}$$

Constitutive equation (Phan-Thien Tanner fluid):

$$K\boldsymbol{\tau}+De\left[\frac{\partial\boldsymbol{\tau}}{\partial t}+\boldsymbol{v}\cdot\nabla\boldsymbol{\tau}-\mathbf{L}\cdot\boldsymbol{\tau}-\boldsymbol{\tau}\cdot\mathbf{L}^T\right]=\frac{De}{De_0}\mathbf{D}. \tag{4}$$

where $\tau_{ij}=\frac{\tau_{ij}\bar{r}_0}{2\eta_0\bar{v}_0},\ K=\exp[2\varepsilon De_0 tr\boldsymbol{\tau}],\ De=De_0\times\exp\left[k(\frac{1}{\theta}-1)\right], De_0=\frac{\lambda_0\bar{v}_0}{\bar{r}_0},\ k=\frac{\bar{k}}{R\theta_0},\ \boldsymbol{L}=\nabla\mathbf{v}-\xi\boldsymbol{D},\quad \boldsymbol{D}=\frac{1}{2}\times(\nabla\mathbf{v}+\nabla\mathbf{v}^T)$.

Equation of energy:

$$\frac{\partial\theta}{\partial t}+\frac{v}{\sqrt{1+(\partial r/\partial z)^2}}\frac{\partial\theta}{\partial z}=-\frac{h_C}{e}(\theta-\theta_a)-\frac{h_R}{e}\left(\theta^4-\theta_a^4\right). \tag{5}$$

where

$\theta=\frac{\bar{\theta}}{\bar{\theta}_0},\ \theta_a=\frac{\bar{\theta}_a}{\bar{\theta}_0},\ \theta_c=\frac{\bar{\theta}_c}{\bar{\theta}_0},\ h_C=\frac{\bar{h}_C\bar{r}_0}{\rho C_p\bar{e}_0\bar{v}_0},\ h_R=\frac{\varepsilon_m\sigma_{SB}\bar{\theta}_0^4\bar{r}_0}{\rho C_p\bar{e}_0\bar{v}_0\bar{\theta}_0},$

$h_C=h_{C0}\left[1+\frac{b(\partial r/\partial z)}{\sqrt{1+(\partial r/\partial z)^2}}\right]\exp[a(\theta-\theta_c)]$.

Boundary conditions:

$$r=1,e=1,v=1,\theta=1,\boldsymbol{\tau}=\boldsymbol{\tau}_0\ \text{ at }\ z=0\ \text{ and }\ t=0 \tag{6a}$$

$$\frac{\partial r}{\partial z}\frac{v}{\sqrt{1+(\partial r/\partial z)^2}}=0, \quad \frac{v}{\sqrt{1+(\partial r/\partial z)^2}}=D_r,$$
$$\theta=\theta_F \text{ at } z=z_F \text{ and } t=0 \quad (6b)$$

where r, e, v, t, and z denote the dimensionless variables of bubble radius, film thickness, fluid velocity, time, and distance coordinate, respectively. ΔP is the difference of air pressures inside and outside the bubble, with B its dimensionless representation. A is the air amount inside the bubble and P_a atmospheric pressure. Other dimensionless variables are: T_z axial tension; θ film temperature, $\boldsymbol{\tau}$ extra stress tensor, $\boldsymbol{\sigma}$ total stress tensor, $\boldsymbol{D}$ strain rate tensor, k activation energy, h_C heat transfer coefficient between the film and the cooling air, an empirical form considering the dependency of h_C on the local conditions of the film (a and b are fitting parameters), h_R radiation coefficient, θ_c the cooling air temperature, and θ_a the ambient temperature. De_0 is the Deborah number, η_0 the zero shear viscosity, and λ_0 the fluid relaxation time under die exit condition. Also, ε and ξ are the PTT model parameters, ε_m the emissivity, σ_{SB} the Stefan–Boltzmann constant, R gas constant, ρ the density, C_P the fluid heat capacity, and D_r the draw ratio. Overlines denote dimensional variables. Subscripts 0, F, and L indicate die exit, freezeline, and nip-roll positions, respectively. Also, subscripts 1, 2, and 3 represent the flow direction, the normal direction, and the circumferential direction, respectively. No further deformation of the film is assumed beyond the freezeline height (FLH, z_F) which was determined by the solidification temperature of a material.[5] Other assumptions have been considered in above equations—dependence of state variables on time and z-coordinate, axisymmetric bubble shape, choice of origin of z-coordinate at the extrudate swell, and no secondary forces (e.g., inertia and gravity forces) and crystallization kinetics.[20]

This work uses the same numerical scheme as reported in Hyun et al.[18] and Shin et al.[20] that involves the orthogonal collocation method on the finite elements of the z-coordinate (OCFE), transforming a free-end time-distance set into a fixed-end time-temperature set through the changeable freezeline height. It has turned out that this OCFE method with the optimal numbers of elements (NE = 5) and inner collocation points (NP = 5), as demonstrated in Figure 2 of Hyun et al.,[18] combining with Newton's method and an implicit 2nd-order backward scheme, guarantees accurate transient dynamics of the state variables. Details for this efficient and robust numerical method are described in the previous literature.[18,20]

For frequency response analysis via transient simulation, a tiny ongoing input or disturbance [eq. (7a)] with preassigned frequency and amplitude was introduced to the steady-state system, resulting in a sinusoidal variation with the same frequency of state variables such as bubble radius and thickness. They would, however, have different amplitudes from the dynamic transient calculation of the above governing equations.

$$Y=Y_s(1+\delta\sin\omega t) \quad \text{at} \quad t>0 \quad (7a)$$
$$\frac{\partial r}{\partial t}+\frac{\partial r}{\partial z}\frac{v}{\sqrt{1+(\partial r/\partial z)^2}}=0, \quad \frac{v}{\sqrt{1+(\partial r/\partial z)^2}}=D_r,$$
$$\theta=\theta_F \text{ at } z=z_F \quad \text{and} \quad t>0 \quad (7b)$$

where Y represents an operating parameter such as take-up velocity (draw ratio, D_r), cooling air temperature (θ_a), heat transfer coefficient (h_{C0}), or air amount inside the bubble (A), which might be an input perturbation in the system with specific amplitude of disturbance (δ) and frequency (ω) from its steady state (Y_s).

To construct neutral stability curves in the BUR-TR diagram, linear stability method described in Lee et al.[19] has been employed, determining the system stability with respect to infinitesimal perturbations from the sign of the real part of the first leading eigenvalue.

RESULTS AND DISCUSSION

A 1% sinusoidal disturbance at take-up velocity, cooling air temperature, heat transfer coefficient, or internal air amount has been introduced to the stable steady-state flow in the frequency domain. Figure 2(a,b) display the one-cycle evolution of the periodic bubble radius and the film thickness profiles when a sinusoidal disturbance with frequency, $\omega = 2.8$ is imposed on take-up velocity, using extensional thickening LDPE data.[20] Transient responses of state variables have different amplitudes and phase lags with the input disturbance, e.g., the amplitude ratio of film thickness at FLH is larger than that of bubble radius in this case [Fig. 2(c)]. Of many possible output responses, amplitude ratio of the film cross-sectional area ($= 2\pi \times r_F \times e_F$) at FLH has been selected to indicate the system sensitivity, representing the change of throughput as in fiber spinning[25,26,28] and film casting.[31]

The amplitude ratio of the output variable relies on the assigned input frequency. Figure 3 exhibits some transient responses and corresponding amplitude ratios of film area at FLH for a wide frequency regime of periodic disturbances introduced to take-up velocity. The frequency at the first peak in the frequency domain is almost equal to the imaginary part of the most leading eigenvalue from the linear stability theory.[27,33]

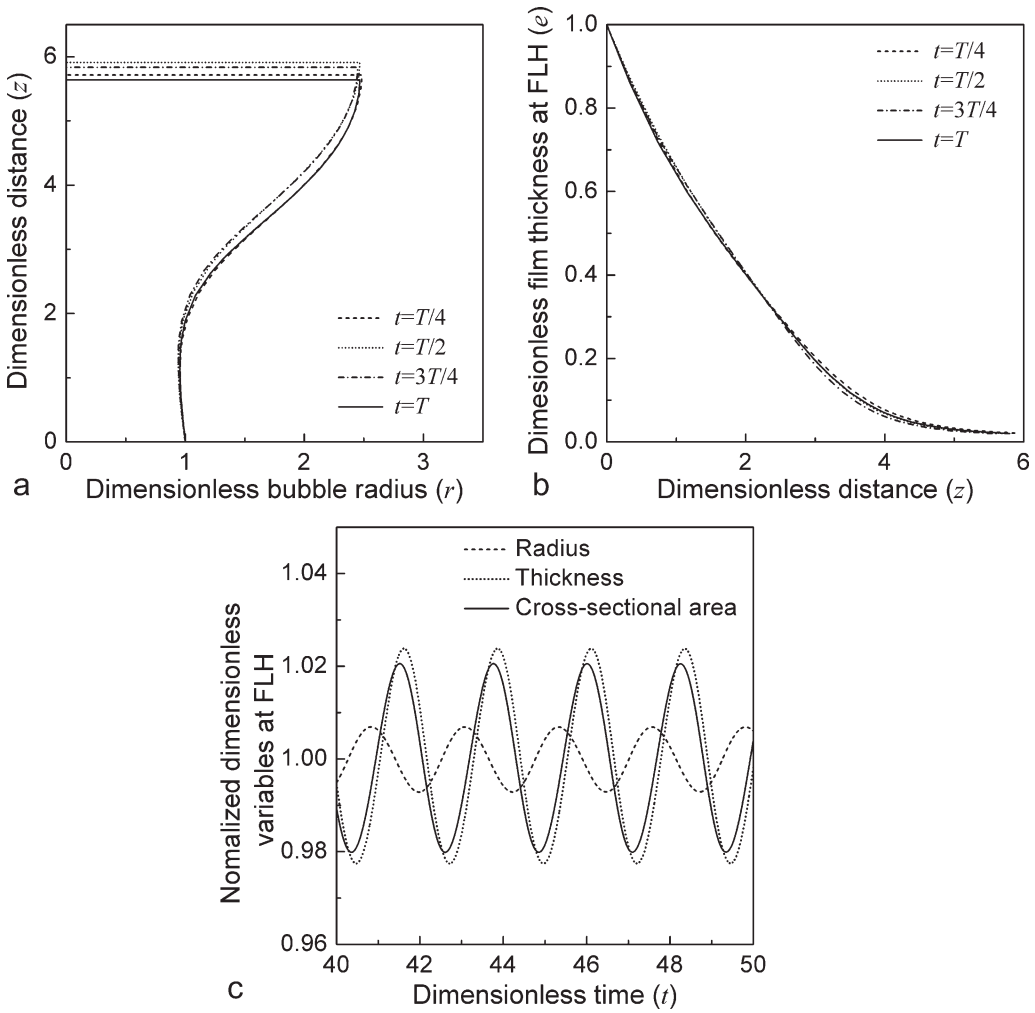

Figure 2 Transient responses of film variables, when a sinusoidal disturbance is introduced to take-up velocity (BUR = 2.465, $D_r = 20$, $De_0 = 0.07$, $\varepsilon = 0.015$, $\xi = 0.1$, $h_{C0} = 0.027$, $\omega = 2.8$, $T = 2\pi/\omega$).

Figure 4 depicts predicted amplitudes of the film cross-sectional area at FLH according to the frequency of sinusoidal perturbations introduced to take-up velocity, heat transfer coefficient, cooling air temperature, and air amount inside the bubble. The different patterns of sensitivity curves depend on the type of disturbance. For instance, a disturbance of take-up velocity produces film of unity amplitude ratio at low frequency, which gradually decreases as frequency increases after the first resonant peak. Whereas, increasing the frequency of perturbations of air amount generally increases the amplitude ratio from a value much less than unity. In agreement with the observations of Jung et al.,[27] ongoing disturbances that change the mass flow rate, e.g., take-up velocity and extrusion velocity, directly altering the output response, give unity amplitude ratio at low frequencies. However, disturbances that do not influence the mass flow rate, e.g., cooling air velocity, cooling air temperature, and air amount inside the bubble, show almost zero amplitude at low frequency.

Comparison of amplitudes at multiple steady states

Changes of amplitude at multiple steady states in nonisothermal cases have been compared (Fig. 5). The multiplicity of steady-state solutions, one of interesting features in the film blowing, is clearly shown in BUR-TR map—two states at the intersection of constant B and D_r lines in isothermal cases[4,16] and three for nonisothermal cases[18,20] [points L, M, H in Fig. 5(a)]. Figure 5(b) shows the amplitude ratio of film area at these three points with respect to a disturbance at take-up velocity. It has been revealed that the middle point is most sensitive to the disturbance. This may be related to the location of the stable steady state in the stability window. Figure 5(c) illustrates the transient variation of film area at

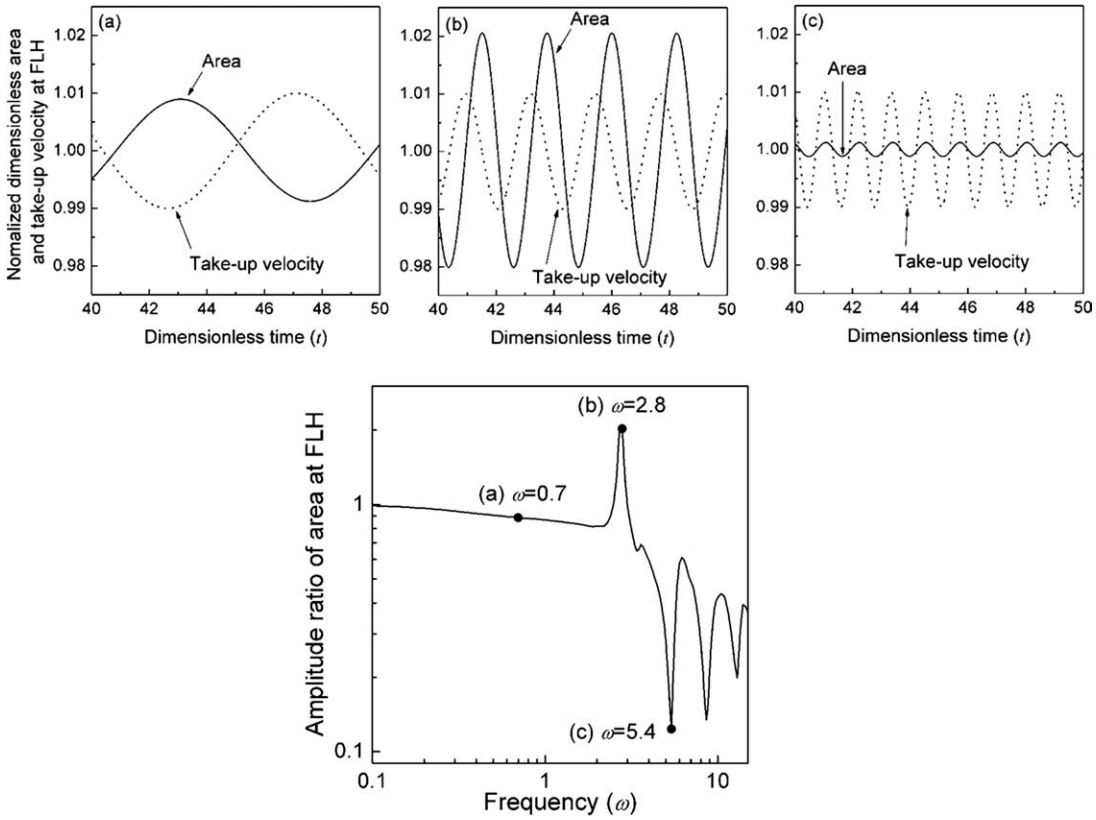

Figure 3 Frequency response of film area at FLH when a sinusoidal disturbance is imposed on take-up velocity (BUR = 2.465, $D_r = 20$, $De_0 = 0.07$, $\varepsilon = 0.015$, $\xi = 0.1$, $h_{C0} = 0.027$).

the three multiple points at FLH when a 1% step change in take-up velocity occurs. Although the system is stable, the middle point appears least stable, taking more computation time to converge to its steady state, indicating that the middle point M near the unstable draw resonance region is more sensitive than the other L and H points. Considering the complexity of film blowing dynamics, further sensitivity results have mainly focused on the middle steady point.

Effect of draw ratio on the sensitivity

The effect of draw ratio on the sensitivity under the same BUR is depicted in Figure 6(a) in which an ongoing disturbance is imposed on the heat transfer coefficient. As draw ratio increases, the steady state shifts towards the unstable draw resonance region [Fig. 6(b)], leading to a system more sensitive to perturbations (higher amplitude ratio of film cross-sectional area at FLH). There is a similar trend in other extensional deformation processes, e.g., fiber spinning and film casting. As draw ratio rises, the first resonance peak progressively moves to a higher frequency, consistent with previous results[26,27] for fiber spinning case, confirming that the frequency at the initial resonance peak is inversely proportional to the fluid residence time. Therefore, increasing D_r for a fixed BUR gives a shorter residence time and a higher frequency at the first peak.

Effect of cooling on the sensitivity

The role of cooling on the stability and sensitivity is portrayed in Figure 7, when a disturbance is

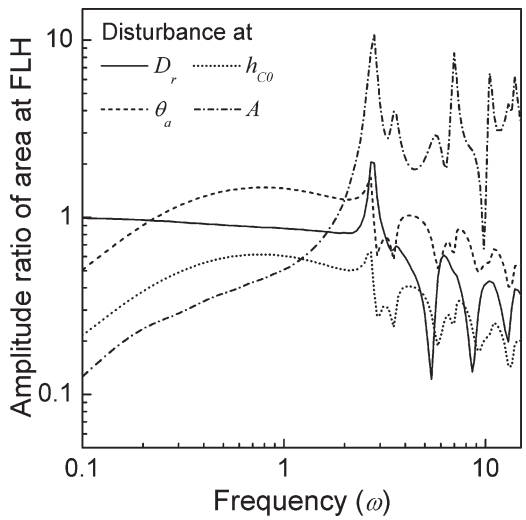

Figure 4 Frequency response of film area at FLH with respect to various disturbances (BUR = 2.465, $D_r = 20$, $De_0 = 0.07$, $\varepsilon = 0.015$, $\xi = 0.1$, $h_{C0} = 0.027$).

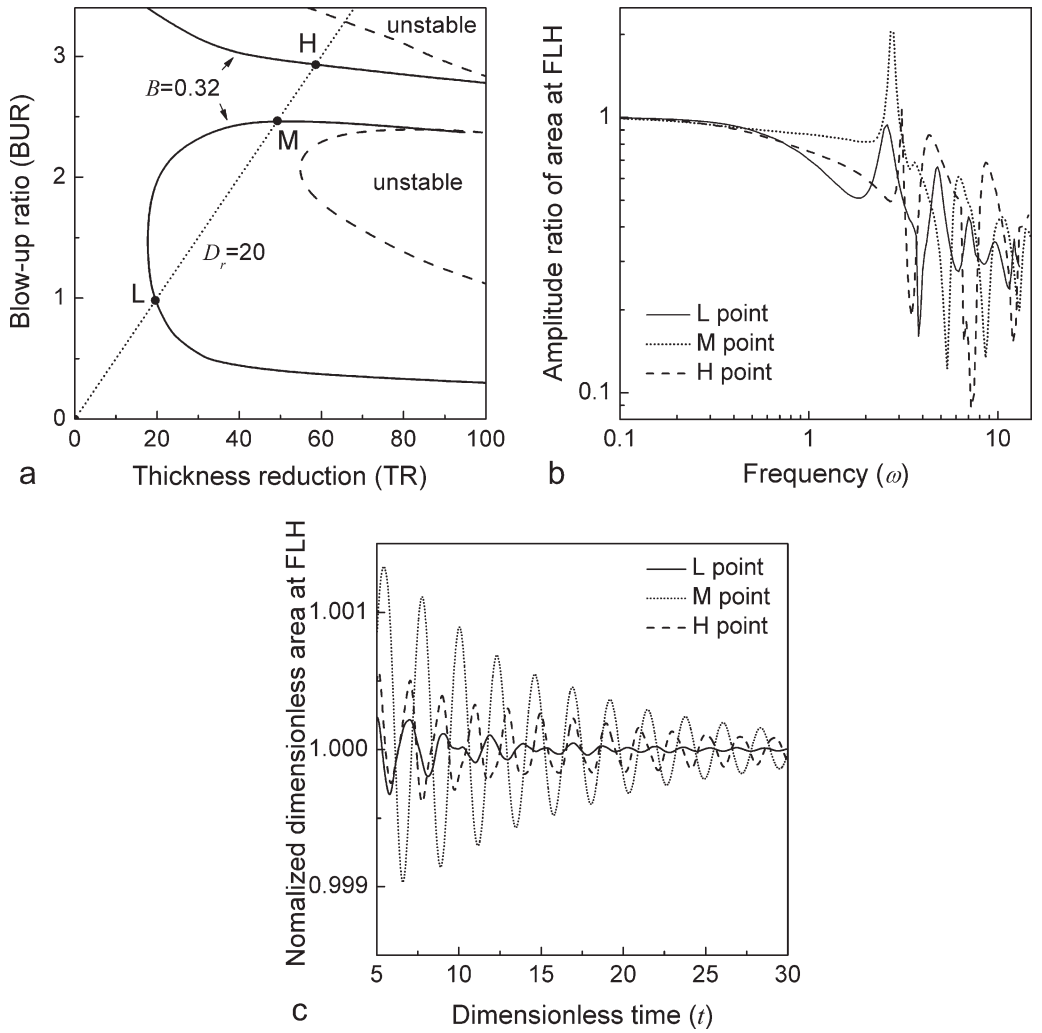

Figure 5 (a) Multiple steady states at $D_r = 20$ and $B = 0.32$, (b) frequency response of film area at FLH with respect to a disturbance in take-up velocity, and (c) transient response of multiple steady states for the step change of take-up velocity ($D_r = 20$, $De_0 = 0.07$, $\varepsilon = 0.015$, $\xi = 0.1$, $h_{C0} = 0.027$).

enforced in heat transfer coefficient. As reported in Jung et al.,[34] cooling always stabilizes the fiber spinning and makes it less sensitive from the transmission linkage with spinline tension. However, cooling is not always positive factor for a stable or insensitive system[19] owing to the more complicated bubble

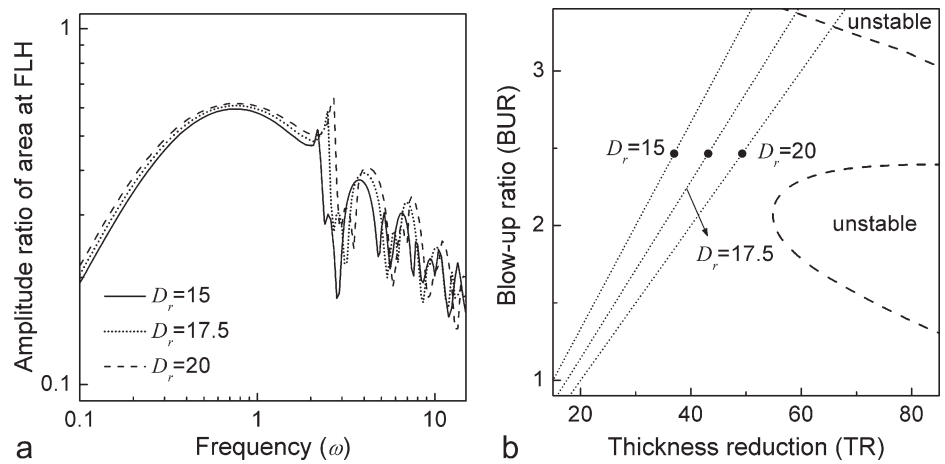

Figure 6 (a) Effect of draw ratio on the sensitivity for a perturbation in heat transfer coefficient and (b) indication of draw ratios in the BUR-TR diagram (BUR = 2.465, $De_0 = 0.07$, $\varepsilon = 0.015$, $\xi = 0.1$, $h_{C0} = 0.027$).

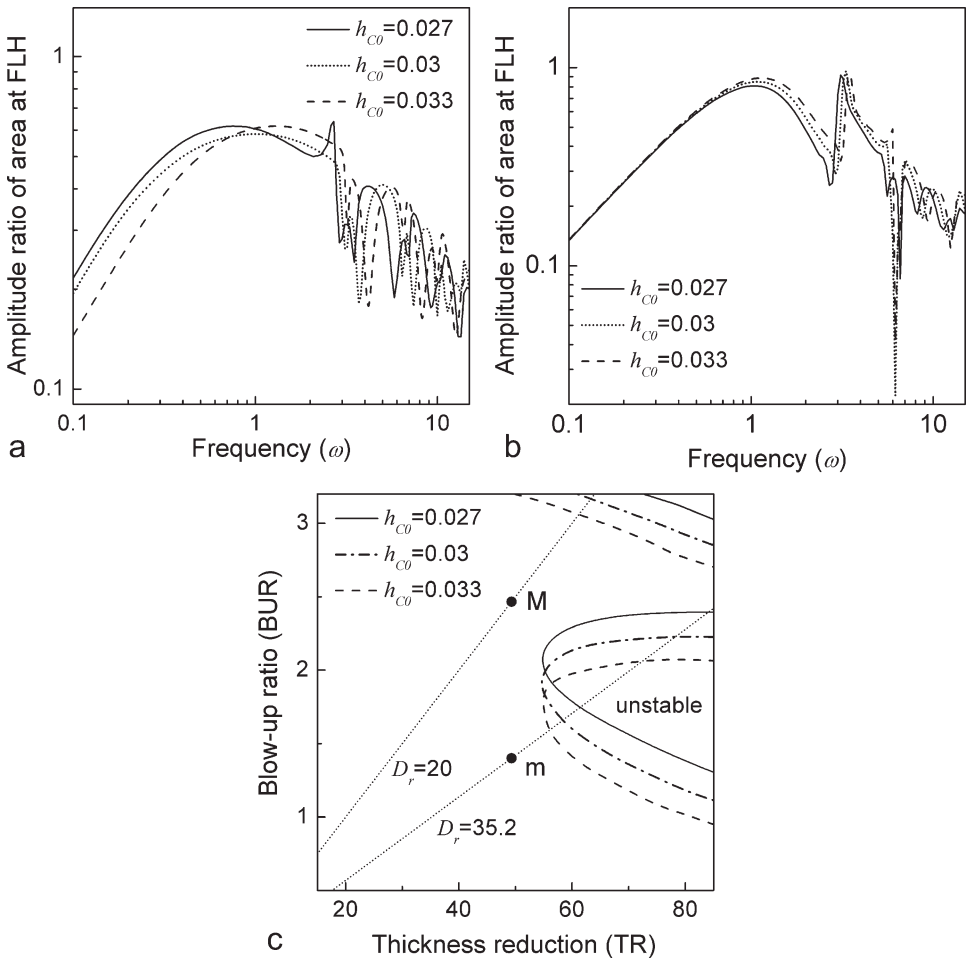

Figure 7 Effect of cooling on the sensitivity at (a) point M ($D_r = 20$, BUR = 2.465) and (b) point m ($D_r = 20$, BUR = 1.4) for a perturbation in heat transfer coefficient and (c) stability in the BUR-TR diagram ($h_{C0} = 0.07$, $\varepsilon = 0.015$, $\xi = 0.1$).

dynamics by the cooling than in the fiber spinning or film casting cases. As cooling is enhanced by increasing heat transfer coefficient (e.g., cooling air velocity), the unstable region in the stability window as well as the freezeline height shifts downwards, making the point M ($D_r = 20$, BUR = 2.465) less sensitive and the point m ($D_r = 35.2$, BUR = 1.4) more sensitive under given conditions.

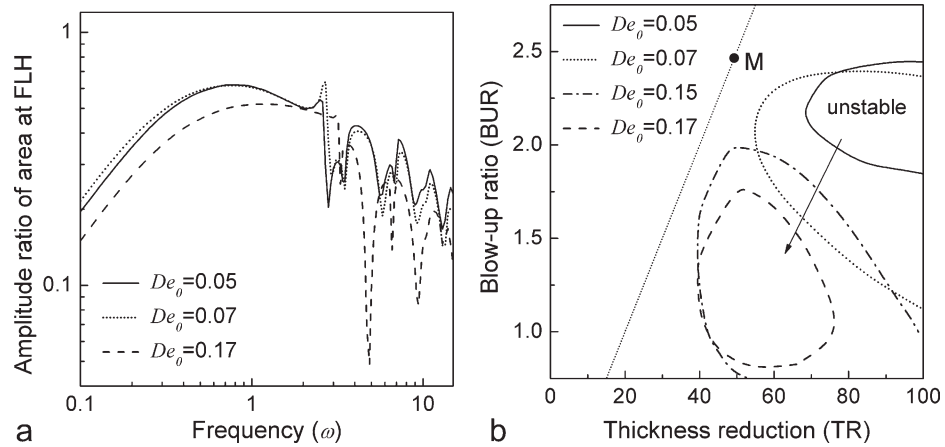

Figure 8 Effect of fluid viscoelasticity on (a) the sensitivity at point M for a perturbation in heat transfer coefficient and (b) stability in the BUR-TR diagram (BUR = 2.465, $D_r = 20$, $\varepsilon = 0.015$, $\xi = 0.1$, $h_{C0} = 0.027$).

Effect of fluid viscoelasticity on the sensitivity

Sensitivity and stability results with fluid viscoelasticity (or *De*) are presented in Figure 8. As in the previous case, a sinusoidal disturbance was introduced to the heat transfer coefficient for the frequency response. It is well known that for the extensional thickening fluids, extensional deformation processes such as fiber spinning and film casting are stabilized and become less sensitive with increased fluid viscoelasticity.[27,35] However, this is not the case for film blowing [Fig. 8(b)]. The unstable region is extended, i.e., the process is destabilized with increasing fluid viscoelasticity at low *De* region (less than about 0.1). At high *De* (higher than about 0.1), the stabilizing effect of viscoelasticity for extensional thickening fluids is exhibited as in other extensional processes, i.e., the system is stabilized with increasing *De*. Therefore, the system is more sensitive to a disturbance at low *De* and thereafter less sensitive at high *De* [Fig. 8(a)].

CONCLUSIONS

The sensitivity of the nonisothermal film blowing process to the various ongoing sinusoidal disturbances has been investigated via transient simulations, incorporating an orthogonal collocation on the finite elements (OCFE). The hyperbolic-like feature of the system makes amplitudes of the film cross-sectional area at freezeline height show resonant peaks with respect to the frequency of the sinusoidal disturbances. Similar to other polymer extensional processes, such as fiber spinning and film casting, the frequency at the first resonant peak corresponds to the imaginary part of the first leading eigenvalue obtained from linear stability analysis. The effects of important process conditions and material properties on the stability and sensitivity have been elucidated. The results show how operating conditions such as draw ratio, blow-up ratio, and cooling affect the process sensitivity. The middle of three multiple steady states exhibits the most sensitive pattern with respect to any disturbance. Viscoelasticity gives the interesting effect of a varied response: for extension thickening fluids it makes the system more sensitive at low *De* and reversely, less sensitive at high *De*.

References

1. Pearson, J. R. A.; Petrie, C. J. S. J Fluid Mech 1970, 40, 1.
2. Pearson, J. R. A.; Petrie, C. J. S. J Fluid Mech 1970, 42, 609.
3. Yeow, Y. L. J Fluid Mech 1976, 75, 577.
4. Cain, J. J; Denn, M. M. Polym Eng Sci 1988, 28, 1527.
5. Andre, J. M.; Demay, Y.; Agassant, J. F. C R Acad Sci II B 1997, 325, 621.
6. Doufas, A. K.; McHugh, A. J. J Rheol 2001, 45, 1085.
7. Fang, Y. L.; Carreau, P. J.; Lafleur, P. G.; Ymmel, S. Polym Eng Sci 2005, 45, 343.
8. Ghaneh-Fard, A.; Carreau, P. J.; Lafleur, P. G. AIChE J 1996, 42, 1388.
9. Henrichsen, L. K.; McHugh, A. J. Int Polym Proc 2007, 22, 179.
10. Henrichsen, L. K.; McHugh, A. J. Int Polym Proc 2007, 22, 190.
11. Muslet, I. A.; Kamal, M. R. J Rheol 2004, 48, 525.
12. Pirkle, J. C.; Braatz, R. D. Polym Eng Sci 2003, 43, 398.
13. Pirkle, J. C.; Braatz, R. D. Polym Eng Sci 2004, 44, 1267.
14. Pirkle, J. C.; Braatz, R. D. J Rheol 2010, 54, 471.
15. Pirkle, J. C.; Braatz, R. D. J Proc Control 2011, 21, 405.
16. Yoon, K. S.; Park, C. W. J Non-Newtonian Fluid Mech 2000, 89, 97.
17. Zhang, Z.; Lafleur, P. G. Polym Eng Sci 2008, 48, 1504.
18. Hyun, J. C.; Kim, H.; Lee, J. S.; Song, H. S.; Jung, H. W. J Non-Newtonian Fluid Mech 2004, 121, 157.
19. Lee, J. S.; Shin, D. M.; Song, H. S.; Jung, H. W.; Hyun, J. C. J Non-Newtonian Fluid Mech 2006, 137, 24.
20. Shin, D. M.; Lee, J. S.; Jung, H. W.; Hyun, J. C. J Rheol 2007, 51, 605.
21. Lee, J. S.; Jung, H. W.; Hyun, J. C. J Rheol 2011, 55, 257.
22. Lee, J. S.; Jung, H. W.; Hyun, J. C. AIChE J 2011 (DOI: 10.1002/aic.12527).
23. Housiadas, K. D.; Klidis, G.; Tsamopoulos, J. J Non-Newtonian Fluid Mech 2007, 141, 193.
24. Denn, M. M. Modeling for Process Control in Adv in Control and Dynamic Systems; Academic Press: New York, 1979.
25. Kase, S.; Araki, M. J Appl Polym Sci 1982, 27, 4439.
26. Devereux, B. M.; Denn, M. M. Ind Eng Chem Res 1994, 33, 2384.
27. Jung, H. W.; Lee, J. S.; Hyun, J. C. Korea-Aust Rheol J 2002, 14, 57.
28. Jung, H. W.; Lee, J. S.; Scriven, L. E.; Hyun, J. C. Korean J Chem Eng 2004, 21, 20.
29. Kohler, W. H.; McHugh, A. J. Chem Eng Sci 2007, 62, 2690.
30. Yun, J. H.; Shin, D. M.; Lee, J. S.; Jung, H. W.; Hyun, J. C. Korean J Chem Eng 2010, 27, 37.
31. Choi, S. W.; Shin, D. M.; Lee, J. S.; Kim, J. M.; Jung, H. W.; Hyun, J. C. Korean J Chem Eng 2009, 26, 26.
32. Phan-Thien, N. J Rheol 1978, 22, 259.
33. Friedly, J. C. Dynamic Behavior of Processes; Prentice-Hall: New Jersey, 1972.
34. Jung, H. W.; Song, H. S.; Hyun, J. C. J Non-Newtonian Fluid Mech 1999, 87, 165.
35. Lee, J. S.; Jung, H. W.; Kim, S. H.; Hyun, J. C. J Non-Newtonian Fluid Mech 2001, 99, 159.